Atomic transport in amorphous $Pd_{40}Ni_{40}P_{20}$ near the glass-transition temperature: Au diffusivity and viscosity

Peter A. Duine, Jilt Sietsma, and A. van den Beukel

Laboratory of Materials Science, Delft University of Technology, Rotterdamseweg 137, 2628 AL Delft, The Netherlands

Measurements of the diffusivity of ion-implanted Au in amorphous $Pd_{40}Ni_{40}P_{20}$ have been performed at temperatures just below the glass-transition temperature. Concentration profiles before and after annealing were determined with Rutherford-backscattering spectrometry. It is found that the diffusivity in as-quenched material decreases to an equilibrium value presumably due to structural-relaxation processes. The equilibrium values of the diffusivity show a very strong temperature dependence and can be described by $D_{eq}(T) = 1.7 \times 10^{17} \exp[-(413 \text{ kJ/mol})/RT] m^2/s$. The results have been quantitatively compared to the viscosity of the same material revealing the breakdown of the Stokes-Einstein relation for this metallic glass. This implies the existence of *two types* of atomic-transport mechanisms in amorphous $Pd_{40}Ni_{40}P_{20}$. Moreover, from cycling between different equilibrium values of the diffusivity, we found that once amorphous $Pd_{40}Ni_{40}P_{20}$ has reached a fully relaxed state, the relation between the viscosity and diffusivity is lost.

I. INTRODUCTION

Should it be expected that, in an amorphous metallic alloy, the Stokes-Einstein relation between the diffusivity and the viscosity is valid? If hydrodynamic flow is responsible for the diffusivity and for the viscosity (i.e., when the mechanism of atomic transport is liquidlike), then the relation between the viscosity and the diffusivity is given by the Stokes-Einstein relation:

$$\eta D = kT/4\pi r , \qquad (1)$$

with $2r$ the atomic diameter, η the viscosity, D the diffusivity, k Boltzmann's constant, and T the temperature. Molecular-dynamics simulations of normal and supercooled liquids[1] indicate, however, that the mechanism of atomic transport changes from hydrodynamic flow to activated jump diffusion as the system is cooled towards the liquid-glass transition. Recent extensions of the mode coupling theory[2] can be invoked to explain why, as the density of the supercooled liquid increases, hydrodynamic flow is no longer active and, ideally, leads to localization of all atoms in a metastable state. It is assumed that already at temperatures *above* the glass-transition temperature "hopping processes" contribute significantly to diffusion and viscous flow.[3] It is therefore expected that a relation between the viscosity and diffusivity in amorphous metallic alloys is not based on hydrodynamic flow, but on these hopping processes. Indeed, in the free volume model for atomic transport,[4] which can nicely be used to describe diffusion and viscous flow in amorphous materials, it is assumed that the diffusivity and viscosity are determined by the same kind of hopping processes. It must be emphasized, however, that the hopping processes for atomic transport in amorphous alloys are not yet well understood.

There are two indications that the hopping mechanism for atomic *diffusion* is of a cooperative, direct type.

(a) The Co diffusivity in amorphous $Co_{76.7}Fe_2Nb_{14.3}B_7$ decreases as a function of time to an equilibrium value, presumably due to structural-relaxation processes.[5] In equilibrium, the Co diffusivity is not a function of pressure and, as estimated from the isotope effect, some ten atoms are involved in the activated jump.[6] These two observations indicate a direct mechanism for atomic diffusion involving some ten atoms in the hopping process.

(b) The Fe diffusivity in amorphous $Fe_{91}Zr_9$ also decreases to an equilibrium value during annealing.[7] Once the material is in equilibrium, temperature changes result in delay-free changes of the Fe diffusivity. This precludes indirect diffusion via quasivacancies in thermal metastable equilibrium if the time scale of the diffusion measurements is smaller than the time scale to establish a new equilibrium vacancy concentration. Furthermore, Kronmüller and Frank[8] argue that the high preexponential factor for Zr diffusion is more in favor of a cooperative hopping mechanism than diffusion via a fixed (i.e., temperature-independent) quasivacancy concentration.

On the other hand, there is also evidence that the hopping mechanism for atomic diffusion is of an indirect, quasivacancy type.

(i) The pressure dependence of crystallization of $Fe_{40}Ni_{40}P_{14}B_6$ measured by Limoge[9] supports a vacancy mechanism since the apparent activation volume equals about one atomic volume.

(ii) Schröder, Samwer, and Köster[10] found Kirkendall voids due to diffusion in an amorphous Zr-Co multilayer.

(iii) Cu and Au diffusion in amorphous $Ni_{50}Zr_{50}$ under irradiation with 1 MeV Kr is enhanced and follows the same characteristics as radiation enhancement of diffusion in crystalline materials.[11] Since it is known that irradiation produces point defects in crystalline solids,

vacancylike defects seem possible as vehicles for diffusion in amorphous $Ni_{50}Zr_{50}$.

A direct cooperative hopping mechanism is certainly in contradiction with diffusion via an indirect quasivacancy mechanism. As suggested by Rätzke, Hüppe, and Faupel,[5] part of the contradiction may arise from different mechanisms in as-quenched and relaxed amorphous alloys. Rätzke, Hüppe, and Faupel found indications from isotope-effect measurements for a single-jump type mechanism for diffusion of Co in *as-quenched* $Co_{76.7}Fe_2Nb_{14.3}B_7$. On annealing, the measurements point to an increasingly cooperative mechanism. This could explain the observation of Kirkendall voids and radiation enhanced diffusion if these observations were obtained in insufficiently relaxed samples. It is unlikely, however, that crystallization occurs in insufficiently relaxed material, which precludes this explanation for the activation volume found from the pressure dependence of crystallisation of $Fe_{40}Ni_{40}P_{14}B_6$.[9]

The mechanism of atomic transport during *viscous flow* has not been studied with such a variety of techniques as the mechanism for atomic diffusion. There are, however, indications that defects in thermal equilibrium play a role in the hopping process. These indications are based on viscosity measurements on relatively stable metallic glasses. In Fig. 1 the experimental results on amorphous $Pd_{40}Ni_{40}P_{20}$ of Ref. 12 represent schematically the behavior of the viscosity of these stable glasses just below the glass-transition temperature. The viscosity of an as-quenched amorphous metal increases during annealing[12-14] [Fig. 1(a)], and eventually reaches a constant value. This equilibrium value is *not* the result of a structurally arrested state, since a subsequent increase of the temperature results in a *non*instantaneous change in the viscosity to a new plateau value [Fig. 1(b)]. Decreasing the temperature to the first annealing temperature shows a noninstantaneous recovery of the viscosity [Fig. 1(c)]. Thus relatively stable metallic glasses (like a-PdNiP) are found to exhibit reversible, *noninstantaneous* changes in the viscosity,[12,14] suggesting the existence of a temperature-dependent equilibrium state. If the viscosity is interpreted with a defect mechanism, the measurements of Fig. 1 indicate that the equilibrium defect concentration is temperature dependent.

In that case, if the mechanism for diffusion is direct and cooperative, it is unlikely that a relation exists be-tween the viscosity and the diffusivity. On the other hand, if the diffusion mechanism is of a quasivacancy type, it may very well be that such a relation does exist. We performed a study of Au diffusion in amorphous $Pd_{40}Ni_{40}P_{20}$ at temperatures just below the glass-transition temperature in order to probe the relation with the viscosity of amorphous $Pd_{40}Ni_{40}P_{20}$.

Amorphous $Pd_{40}Ni_{40}P_{20}$ was chosen because of its high stability which allows us to study atomic transport around the glass-transition temperature. Therefore, we can test the relation between the viscosity and diffusivity in as-quenched material, in equilibrium, and, on changing the temperature after equilibrium has been attained, during the transition from one equilibrium value to an other. We will show that the possibility of cycling between different equilibrium values yields important information on the relation between the viscosity and diffusivity. Furthermore, already quite a few investigations of the relation between the diffusivity and viscosity have been performed in amorphous alloys at temperatures *well below* the glass-transition temperature. Some of these studies used multilayers and indicated the validity of the Stokes-Einstein relation[15,16] but with a surprisingly low value of *r*. Other work indicated the break-down of the Stokes-Einstein relation: van den Beukel compared the viscosity of $Fe_{40}Ni_{40}B_{20}$ measured by van den Beukel *et al.*[17] and the Fe diffusivity in $Fe_{40}Ni_{40}B_{20}$ measured by Horváth and Mehrer[18] and showed that part of Horváth and Mehrer's data could be related to the viscosity with a supplant for the Stokes-Einstein relation.[19] By using multilayers, Witvrouw[20] also showed the breakdown of the Stokes-Einstein relation and found a good description of her data with the supplant for the Stokes-Einstein relation proposed by van den Beukel.[19] The present study in amorphous $Pd_{40}Ni_{40}P_{20}$ is especially suited for testing the Stokes-Einstein relation or its supplant just below the glass-transition temperature where the equilibrium viscosity can be attained.

We have chosen Rutherford-backscattering spectrometry (RBS) to determine the Au concentration profiles. This technique has the advantage of a good accuracy, and most importantly, the method is non-destructive. This, together with the high stability of amorphous $Pd_{40}Ni_{40}P_{20}$, allows several reanneals at different temperatures and determinations of concentration profiles of a single sample.

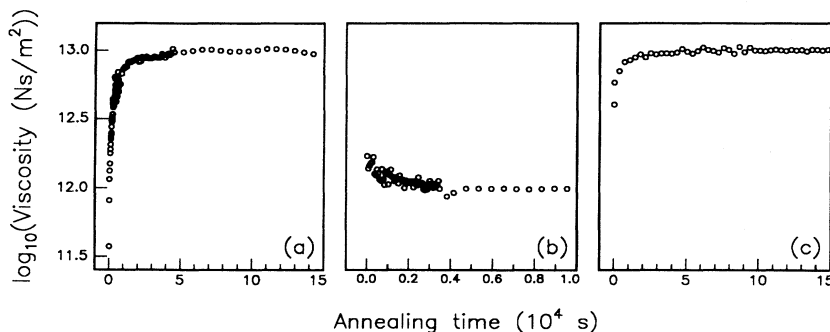Au was chosen because it is ideally suited for RBS

FIG. 1. A schematic representation of the results of viscosity measurements from Ref. 12. In (a) the viscosity of as-quenched material is measured at 553 K, in (b) the temperature was raised to 563 K and in (c) it was decreased to the first annealing temperature.

analyses. Furthermore, owing to quite a few systematic studies of the size dependence of the diffusion species in amorphous alloys [e.g., in amorphous $Fe_{40}Ni_{40}B_{20}$ (Ref. 21) and in amorphous $Pd_{78}Cu_6Si_{16}$ (Ref. 22)], correlations between the diffusion and the size ratio of the major constituents and the tracer atoms have been proposed,[21] suggesting that Au, which is only slightly bigger than Pd, diffuses by the same mechanism as Pd. This is important in the study of a possible relation with the viscosity, since the low-mobility atom Pd is expected to determine the viscosity.

II. EXPERIMENT

The alloy was composed in an argon atmosphere from elemental Pd and Ni_2P of 99.9% purity. Amorphous ribbons were obtained by the melt-spinning technique[12] and the initial Au concentration profiles were obtained by a 20 keV ion implantation in the shiny side of the ribbons.[23] We used ion implantation because it provides an intimate contact with the host material. This circumvents surface hold up which is frequently observed when the diffusion species is evaporated on the surface of the ribbons. Such an effect is usually ascribed to oxidation or difficulties in dissolving the diffusion species.

In order to reduce compositional effects on the diffusivity and to minimize the radiation damage from the implant, Au was implanted to a low dose of 0.8×10^{15} at/cm^2. The implant resulted in a Gaussian depth distribution of Au with an average straggling of 0.7 nm and a mean projected range of 2.2 nm. At the mean projected range, the Au concentration was 5 at. %. It should be noted that detectable radiation-enhanced diffusion usually occurs at much higher doses and implantation energies.[11,24]
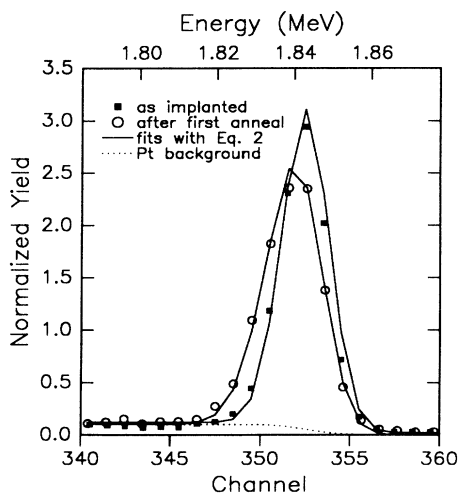

FIG. 2. RBS measurements of Au concentration profiles, obtained after 20 keV, 0.8×10^{15} at/cm^2 implantation (squares) and after subsequent annealing at 545 K for 117 000 s (circles). Solid lines are fits with Eq. (2). The dotted line gives the background signal from a Pt contamination in the host material (Ref. 23).

The concentration profiles before and after diffusion were determined with Rutherford-backscattering spectrometry using a 2 MeV He^+ beam and measuring the energy of the backscattered helium particles at an angle of 170° from the incident beam. A typical as-implanted RBS spectrum (Au part only) is shown in Fig. 2.

Consecutive diffusion anneals were carried out in an open-ended tube furnace with a flowing helium atmosphere. For each treatment the annealing times were about 500 s at the highest annealing temperature (585 K) and about 100 000 s at the lowest annealing temperature (545 K). After annealing, the samples were checked for crystallinity by standard x-ray-diffraction measurements. The glass-transition temperature of the unimplanted ribbons as measured by a differential scanning colorimetry (DSC) experiment at 20 K/min is 585 K. A typical result of the widening of the concentration profile during an annealing treatment is given in Fig. 2. The full lines are fits with

$$n(x,t_D) = \frac{N_T}{R_s(t_D)\sqrt{2\pi}} \left[\exp\left[-\frac{(x-R_m)^2}{2R_s^2(t_D)} \right] + \exp\left[-\frac{(x+R_m)^2}{2R_s^2(t_D)} \right] \right], \quad (2)$$

with $n(x,t_D)$ the amount of Au at a depth x from the surface of the specimen after annealing during t_D. The second term in Eq. (2) accounts for reflection of the Au atoms at the surface of the specimen.[25] For each sample the implanted dose N_T and the mean projected range R_m are fixed. Therefore, $R_s(t_D)$, the width after a diffusion annealing time t_D, is the only free parameter to fit the RBS spectra. In the example presented in Fig. 2, the initial straggling of the concentration profile changes from 0.7 nm to a width of 3.6 nm after annealing for $t_D = 117\,000$ s at 545 K. The profiles are broadened with a resolution function with a full width at half maximum of 14 keV.[23]

In all cases, Eq. (2) yielded good fits to the Au parts of the RBS spectrum, even after seven reanneals which increased the width from 0.7 to 12 nm. If the initial concentration profile would have differed widely from a Gaussian profile these good fits were highly improbable. In addition, this makes it unlikely that concentration-dependent diffusion, radiation-enhanced diffusion in the region of the Au implant, and contamination with oxygen or other elements greatly influence the diffusion. Time-dependent diffusivity is accounted for by the average value of the diffusivity,

$$\bar{D} = \frac{\int_0^{t_D} D(t)dt}{t_D}, \quad (3)$$

which can be obtained by a comparison of the width of different concentration profiles:

$$\bar{D} = \frac{R_s^2(t_D) - R_s^2(0)}{2t_D}, \quad (4)$$

as follows directly from Fick's law. The inaccuracy of the diffusivities was assumed to result mainly from the

counting statistics in the RBS measurements. In that case, sharper profiles yield better accuracies. Equation (4) implies that long annealing times improve the accuracy of $\bar{D}$. This was effectuated in the determination of the equilibrium diffusivities, but the time dependence of the diffusivity could only be shown by limiting t_D.

III. RESULTS

A. The diffusivity of Au

In Fig. 3 the results of diffusion measurements at 545 K of Au implanted in *as-quenched* amorphous $Pd_{40}Ni_{40}P_{20}$ are shown by the open symbols, showing a reduction of the diffusivity from 11.5×10^{-23} m^2/s measured during the first annealing treatment to a constant value of 4×10^{-23} m^2/s. The decreasing diffusivity is most likely not the result of annealing out of radiation damage due to the Au implant. This can be seen from the full symbols presented in Fig. 3. Here the diffusivity at 545 K was measured in a *preannealed* specimen (273 600 s at 550 K prior to the implantation). It is clear that in this case no decrease in $\bar{D}$ is found, which rules out significant radiation-enhanced diffusion. Both sets of measurements (preannealed and as-quenched) yield a stabilized value of the diffusivity at 545 K of $D_{eq}(545$ $K)=4 \times 10^{-23}$ m^2 /s.

In Fig. 4 it is shown that the diffusivity of Au in as-quenched amorphous $Pd_{40}Ni_{40}P_{20}$ decreases to $D_{eq}(553$ $K)=1.6 \times 10^{-22}$ m^2/s during annealing treatments at 553 K. In order to investigate the plateau values of the diffusivity more carefully, several annealing treatments were given after the diffusivity reached the plateau value. Since in this case the diffusivity does not change during the annealing treatment, $\bar{D}=D_{eq}$ for any combination of concentration profiles. This was used for six different
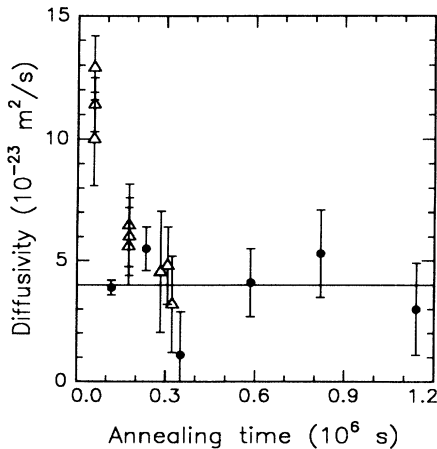

FIG. 4. Time-dependent diffusivity of ion-implanted Au in as-quenched amorphous $Pd_{40}Ni_{40}P_{20}$ at 553 K. The solid line gives $D_{eq}(553$ K).

temperatures between 545 and 585 K. As an example in Fig. 5 the stabilized diffusivity at 575 K is shown resulting from five concentration profiles after reaching equilibrium. It is shown that, as expected [Eq. (4)], the accuracy of the diffusivity improves with the accumulated annealing time.

The equilibrium diffusivities for six different temperatures are plotted in an Arrhenius graph in Fig. 6. The temperature dependence of the equilibrium diffusivities were related to

$$D_{eq}(T)=D_0^* \exp(-Q^*/RT) , \qquad (5)$$

and can be described by an activation energy $Q^*=413$ kJ/mol and a pre-exponential factor $D_0^* =1.7 \times 10^{17}$ m^2/s. These are fairly high values as compared to

FIG. 3. Time-dependent diffusivity of ion-implanted Au in amorphous $Pd_{40}Ni_{40}P_{20}$ at 545 K. Open symbols refer to samples which were in the as-quenched state when the Au was implanted. The full symbols are measured on a specimen which was pre-annealed at 550 K prior to the implantation. The solid line gives the stabilized value of the diffusivity.
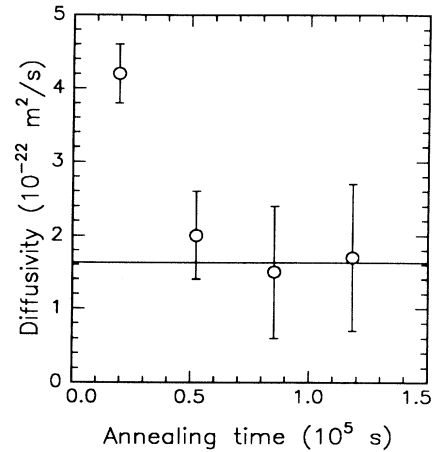
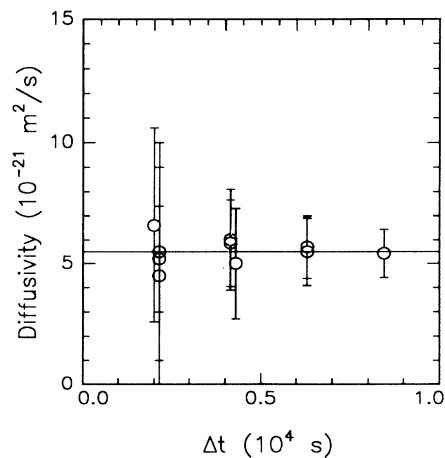

FIG. 5. Equilibrium diffusivity at 575 K of Au in amorphous $Pd_{40}Ni_{40}P_{20}$ measured on *one* sample. The ordinate plots the difference in annealing time between the measurements of the Au concentration profile.
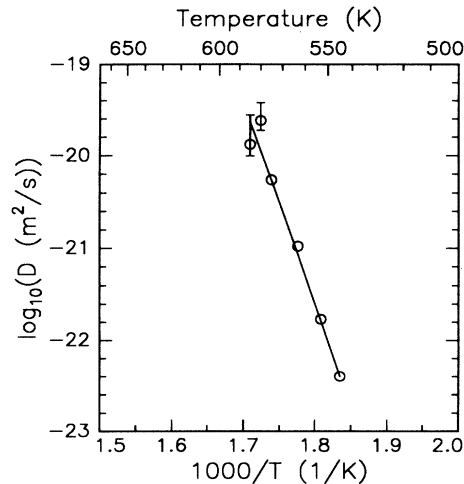
FIG. 6. An Arrhenius graph of the equilibrium diffusivities of Au in amorphous $Pd_{40}Ni_{40}P_{20}$. The error bars indicate the accuracy of the diffusivities that were determined in the way shown in Fig. 5. For the data measured between 545 and 575 K, the error bars are smaller than the symbol size.

FIG. 8. Time-dependent diffusivity at 545 K in as-quenched samples (open symbols) and *instantaneous* changes in the diffusivity from the equilibrium value at 580 K to the equilibrium value at 545 K (closed symbols). The solid line gives D_{eq}(545 K).

diffusion in crystalline materials and in the amorphous materials studied so far.[26]

The strong temperature dependence of D_{eq} could reflect the temperature-dependent equilibrium state as revealed by the viscosity measurements. The definite proof that the equilibrium structure changes upon changing the temperature was formed by the time dependence of the viscosity after changing from the equilibrium state at one temperature to another. In Fig. 3 a time-dependent diffusivity was shown at $T=545$ K but only when departing from the as-quenched state. Changing from $T=550$ K to 545 K (also in Fig. 3) is likely to be too small a change in temperature to detect a possible time dependence of the diffusivity. Therefore, two sets o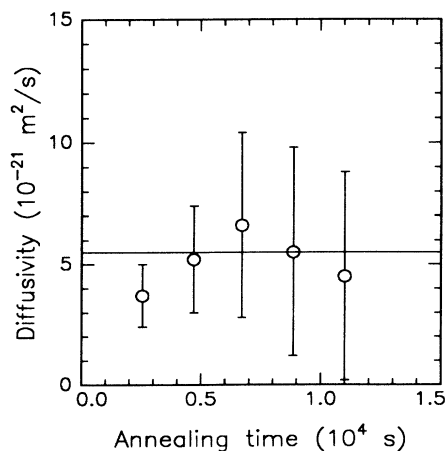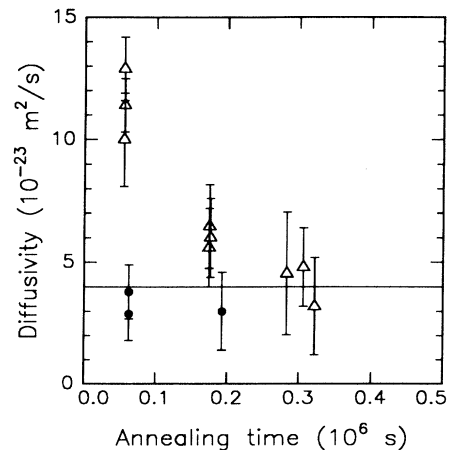f experiments were performed in order to show the time dependence of the diffusivity upon changing from the equilibrium state at one temperature to another.

(a) We aimed at an increasing diffusivity by first stabilizing at the low temperature $T=545$ K, and subsequently measuring the diffusivity at the high temperature $T=575$ K. The results of these measurements are shown in Fig. 7. Although the first data point is slightly lower than the rest, the accuracy is not sufficient to consider this effect significant.

(b) The second series aimed at a decreasing diffusivity by changing to a lower temperature. In order to optimize the accuracy, the samples were equilibrated for 1000 s at $T=580$ K before the Au implantation. The diffusivity was measured at $T=545$ K. The results are given in Fig. 8, together with the as-quenched results from Fig. 3. Where, in the case of diffusion related to a temperature-dependent equilibrium state we would expect a decrease of the diffusivity comparable to the decrease observed in the as-quenched specimens, the first point already yields the equilibrium diffusivity of 4×10^{-23} m²/s. This remarkable difference from the behavior of the viscosity will be discussed in the next section.

B. The relation between diffusivity and viscosity

In this section a possible relation between the diffusivity and the viscosity will be discussed based on the present experimental data for the diffusivity and the experimental data for the viscosity that were presented in the Refs. 12 and 27. A model-based discussion of this relation will be given in Sec. IV.

The Stokes-Einstein relation, presented in the Introduction, proposes a connection between the diffusivity and the viscosity of liquids, and possibly also for under-cooled liquids. It implies a linear temperature dependence of the product ηD [Eq. (1)]. For the equilibrium values the Stokes-Einstein relation is tested in Fig. 9.
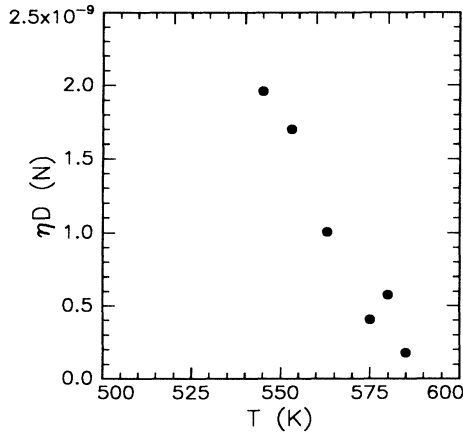

FIG. 7. Measurements of the diffusivity at 575 K after equilibration of the sample at 545 K. The solid line gives D_{eq}(575 K) (see Fig. 5).

FIG. 9. The Stokes-Einstein product (ηD) for amorphous $Pd_{40}Ni_{40}P_{20}$. Only the equilibrium values of the diffusivity and viscosity (Ref. 27) are shown.
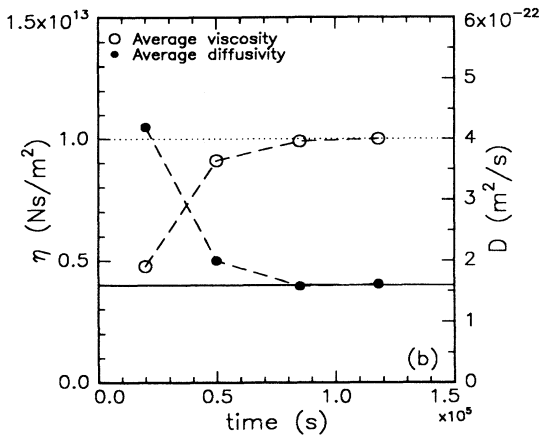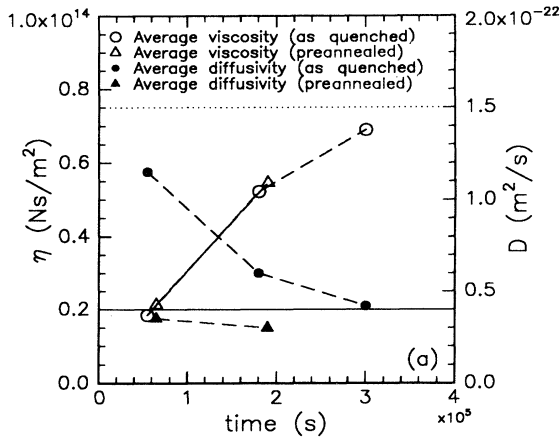

FIG. 10. Time-dependent diffusivity and viscosity at (a) 545 K and at (b) 553 K for samples initially in the as-quenched state (closed and open circles, respectively). The solid and open triangles in (a) refer respectively to the diffusivity and viscosity for specimens previously annealed at 580 K.

Within the accuracies a linear relation is possible, but the negative value of the slope is unphysical [cf. Eq. (1)]. Figure 9 therefore shows that the Stokes-Einstein relation is not valid in the fully relaxed state of the glass. It should be noted that the influence of Au being slightly larger than Pd would be a more positive slope in Fig. 9 if a simple quasivacancy mechanism is assumed.

By averaging the viscosity data over the annealing times used for the diffusivity experiments, the time dependence of $\overline{D}$ and $\overline{\eta}$ in isothermal experiments can be compared. Figure 10(a) gives these data for $T=545$ K and Fig. 10(b) for $T=553$ K (diffusivity data of the Figs. 3 and 4). Clearly a relation exists between $\overline{D}$ and $\overline{\eta}$ during the transition from the as-quenched to the equilibrium state (open and solid circles). The annealing time characterizing this transition is the same for both properties, which suggests that one process is responsible for the decreasing diffusivity and for the increasing viscosity. However, again no Stokes-Einstein relation is found. Evaluating the data, it turns out that ηD is not constant at each temperature, but ηD^2 is. This will be discussed extensively in Sec. IV.

Once the equilibrium state is reached, however, the relation between diffusivity and viscosity is lost, as is evidenced by the open and solid triangles in Fig. 10(a). These data refer to experiments at $T=545$ K, performed on specimens that were previously equilibrated at $T=580$ K. The viscosity shows an increase that is fully compatible with the data for the as-quenched specimens, but the diffusivity behaves completely different. $\overline{D}$ shows a time-independent value that coincides with the equilibrium value at $T=545$ K. So, whereas for the viscosity the as-quenched state might be described as the equilibrium state for a temperature close to 580 K, such a description is impossible with regard to the diffusivity. A significant difference seems to exist between the relaxation process from the as-quenched state and the relaxation process between equilibrium states, the former affecting both η and D, the latter only η.

IV. DISCUSSION

To analyze the present data more precisely, we will introduce the free volume theory which offers an explanation for the temperature dependence of the viscosity and diffusivity. The free volume theory[4] assumes a defect mechanism for atomic transport with, in equilibrium, a temperature-dependent defect concentration $c_{f,\mathrm{eq}}$ which is given by a Fulcher-Vogel type equation:

$$c_{f,\mathrm{eq}}=\exp[-B/(T-T_0)] , \qquad (6)$$

where B and T_0 are constants. The approach to equilibrium, both for as-quenched and for preannealed samples, can be described by production and annihilation processes of defects (see Ref. 12):

$$\frac{dc_f}{dt}=-k_r c_f(c_f-c_{f,\mathrm{eq}}) , \qquad (7)$$

with k_r a rate constant, c_f the actual defect concentration, and $c_{f,\mathrm{eq}}$ given by Eq. (6). Spaepen[28] derived, start-

ing from the ideas developed for diffusion and viscous flow in crystalline materials, the relation between the two atomic-transport coefficients and the defect concentration in amorphous metals:

(a) The diffusivity can be given by

$$D = \lambda_D^2 fck_D c_D ,$$ (8)

with λ_D the jump distance, fc the product of a correlation factor and a geometric factor (usually on the order of one for crystalline materials), k_D the jump frequency $[k_D = \nu_D \exp(-Q_D/RT)$, with ν_D the attempt frequency and Q_D the migration activation energy], and c_D the concentration of defects that can be used as diffusion vehicles.

(b) The relation between the viscosity and the defect concentration is given by

$$\eta = \frac{kT\Omega}{k_f(\gamma_0 v_0)^2 c_f} ,$$ (9)

with k_f the jump frequency $[k_f = \nu_f \exp(-Q_f/RT)$ with ν_f the attempt frequency and Q_f the migration activation energy for viscous flow], v_0 the volume of a defect for viscous flow, γ_0 the shear strain per jump, c_f the concentration of defects that can be used as vehicles for viscous flow, and Ω the atomic volume.

The product of the two atomic-transport coefficients is given by the Stokes-Einstein relation [Eq. (1)], with

$$r = \frac{(\gamma_0 v_0)^2}{\Omega fc\lambda^2} \frac{k_f}{k_D} \frac{c_f}{c_D} .$$

In the Spaepen model, c_D and c_f are structure-dependent quantities and these are calculated using Eqs. (6) and (7). Spaepen assumes c_D and c_f to be proportional to one another and therefore r should be constant during an isothermal experiment.

A nonproportional relation between the defects connected to the viscosity and the diffusivity has been suggested by van den Beukel.[19] van den Beukel assumes that a pair of defects is required for atomic transport during viscous flow, whereas only one is needed for atomic transport for diffusion. Mathematically, this gives rise to a constant ratio c_f/c_D^2. This means that at constant temperature ηD^2 is constant, as can be seen from Eqs. (8) and (9). Again, c_D and c_f are structure dependent and are calculated using Eqs. (6) and (7). This supplant for the Stokes-Einstein equation nicely relates part of the measurements of the viscosity of $Fe_{40}Ni_{40}B_{20}$ by van den Beukel et al.[17] and ^{59}Fe diffusivity measurements by Horváth and Mehrer.[18]

Since the present diffusivity data were measured on the same material as the viscosity data in Refs. 12 and 27, and the parameters of the free volume model were determined from these viscosity data, a quantitative test of the two above-mentioned relations can be made. Use of either $c_D(t,T) \propto c_f(t,T)$ ($\Longrightarrow \eta D = $const) or $c_D^2(t,T) \propto c_f(t,T)$ ($\Longrightarrow \eta D^2 = $const) gives the time and temperature dependence of $D(t,T)$. The proportionality factor between η and c_f was determined from a fit with Eq. (9)

to the complete set of data from Ref. 12. The proportionality factor between D and c_D [Eq. (8)] is obtained from the value of $D_{eq}(545$ K$)$, assuming $c_D = c_f$ or $c_f = c_D^2$.

The two suggested relations between η and D were evaluated on three points.

Time-dependent diffusivity in as-quenched material. The average diffusivity during an annealing treatment of as-quenched $Pd_{40}Ni_{40}P_{20}$ at 545 K was measured to be $11.5 \pm 1.5 \times 10^{-23}$ m^2/s (Fig. 3). Calculation of this data point yields $\bar{D} = 60 \times 10^{-23}$ m^2/s if $\eta D = $const, and $\bar{D} = 10 \times 10^{-23}$ m^2/s if $\eta D^2 = $const.

Equilibrium diffusivities. Using either of the two models, part of the temperature dependence of D_{eq} is described with a temperature-dependent defect concentration [Eq. (6)] as determined from the viscosity measurements. Describing the data of Fig. 6 with Eqs. (6) and (8) implies $Q_D = 20$ kJ/mol if ηD is assumed to be constant, and $Q_D = 220$ kJ/mol if $\eta D^2 = $const.

Jump distance. Under the assumptions $\nu_D = \nu_f$, $fc = 1$, and Q_D as determined from the equilibrium diffusivities, the equilibrium diffusivities can be used to calculate λ_D. For $\eta D = $const, $\lambda_D = 3.6 \times 10^{-7}$ nm is found. For $\eta D^2 = $const, we find $\lambda_D = 0.23$ nm.

In all three respects the supplant for the Stokes-Einstein equation,[19] suggesting $\eta D^2 = $const and $c_f = c_D^2$, yields far more realistic values.

The experiments of the Figs. 7 and 8 investigated the change in diffusivity upon changing the temperature for fully relaxed material. In Fig. 7 (temperature change $545 \rightarrow 575$ K) both the Stokes-Einstein relation and the supplant $\eta D^2 = $const predict a value $D = 4.5 \times 10^{-21}$ m^2/s for the data point at an annealing time of 2700 s, which is only 20% lower than the equilibrium value. Although the measured value is in agreement with this result, the accuracy is not sufficient to detect the time dependence of D that results from the time dependence of η.

Also the temperature change $580 \rightarrow 545$ K has been investigated. On this temperature change the change in viscosity is virtually identical to the change in η for an as-quenched sample [Fig. 10(a), open circles and triangles]. For the as-quenched case the data can be well described by $\eta D^2 = $const. Both in Figs. 8 and 10(a) the diffusivity for the 580 K preannealed samples is significantly lower than for the as-quenched samples. It can therefore not be described by either $\eta D = $const or $\eta D^2 = $const. More generally, any relation between η and D seems to be lost, since D remains constant in a regime where η changes significantly. An important point might be that the Au diffusion takes place very close to the surface of the sample (maximum depth on the order of 20 nm). This may result in kinetics of defect annihilation and production different from that in the bulk. Also, the results might be influenced by surface contamination or surface crystallization. However, these aspects influence the "as-quenched" and the "580 K" data in Fig. 8 in a similar manner, and can therefore not be the cause of the

large difference.

The picture that emerges from the present measurement suggests that in the as-quenched state, and during relaxation towards equilibrium, the mechanism of atomic transport is of a quasivacancy type, as suggested by the free-volume theory. The results for the preannealed samples, where the relation between the viscosity and diffusivity is lost, perhaps indicate a change in atomic transport mechanism for diffusion similar to the change found by Rätzke, Hüppe, and Faupel[5] from isotope-effect measurements. These measurements pointed to a change from an indirect quasivacancy mechanism towards a direct cooperative mechanism upon annealing.

Similar results were reached by Horváth et al.[7] on the diffusion of Fe in amorphous $Fe_{91}Zr_9$. From the as-quenched state a time-dependent diffusivity was found, resulting in an equilibrium value. Upon changing the temperature, instantaneous changes of D suggest a temperature dependence of the atomic mobility only, and not of the equilibrium structure. The FeZr measurements were performed at temperatures well below the glass-transition temperature. The present study on $Pd_{40}Ni_{40}P_{20}$ has been performed at temperatures very close to the glass-transition temperature, where it has been found previously that a temperature-dependent equilibrium state is indicated not only by the viscosity,[12,27] but also by the speed of sound[29] and the glass transition as seen by differential scanning calorimetry.[30]

Surprisingly, the supplant for the Stokes-Einstein relation ($c_f \propto c_D^2$) used to calculate ηD for higher temperatures than the glass-transition temperature, yields an agreement with the experimental data collected by Rössler[31] for tri-α-naphtyl benzene. As an example, in Fig. 11 experimental data are shown of the Stokes-Einstein product together with the calculated Stokes-Einstein product for amorphous $Pd_{40}Ni_{40}P_{20}$.

Furthermore, Knuyt, Stals, and de Schepper[26] found, when the diffusivities in quite a number of unstable glasses are related to the temperature by Eq. (5), that the apparent pre-exponential factor D_0^* and the apparent activation energy Q^* are related. It was found that a high activation energy is connected to a high pre-exponential factor. The authors explain this relation by a *distribution* of activation energies governing the activated direct diffusion process. An alternative explanation for this relation is the temperature dependence of the equilibrium defect concentration [Eq. (6)] as formulated by the free volume theory.[4] When mapped on Eq. (5), this temperature dependence affects both D_0^* and Q^*. With B and T_0 from the viscosity measurements[12] and using $\eta D^2 = const$, the order of magnitude of the variations in
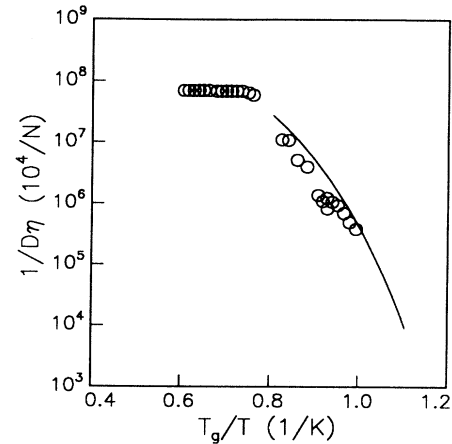

FIG. 11. The Stokes-Einstein product for tri-α-naphtyl benzene [data taken from Rössler (Ref. 31)], and calculated for amorphous $Pd_{40}Ni_{40}P_{20}$ in equilibrium (solid line) using $c_f = c_D^2$.

D_0^* and Q^* is the same as Knuyt, Stals, and de Schepper[26] found with realistic values of the activation energy spectrum.

V. CONCLUSIONS

It was shown that the diffusivity of ion-implanted Au in as-quenched amorphous $Pd_{40}Ni_{40}P_{20}$ is time dependent in isothermal experiments. The diffusivity relaxes to an equilibrium value which is strongly temperature dependent. The nice agreement with the time dependence of the viscosity suggests a single relaxation process for the change in these atomic-transport coefficients. It turned out, however, that once the equilibrium diffusivity is reached, the diffusivity is decoupled from this relaxation process, which means that the relation between the viscosity and diffusivity is lost.

ACKNOWLEDGMENTS

[1]J. L. Barrat, J. N. Roux, and J. P. Hansen, Chem. Phys. **149**, 197 (1990); G. Wahnström, Phys. Rev. A **44**, 3752 (1991); L. J. Lewis, Phys. Rev. B **44**, 4245 (1991).

[2]For a review, see L. Sjögren and W. Götze, in *Dynamics of Disordered Materials*, Vol. 37 of Springer Proceedings in Physics, edited by D. Richter, A. J. Dianoux, W. Petry, and J. Teixeira (Springer, Berlin, 1989), p. 18.

[3]S. P. Das and G. F. Mazenko, Phys. Rev. A **34**, 2265 (1986); W. Götze and L. Sjögren, Z. Phys. B Condensed Matter **65**, 415 (1987).

[4]D. Turnbull and M. H. Cohen, J. Chem. Phys. **29**, 1049 (1958); M. H. Cohen and D. Turnbull, *ibid.* **31**, 1164 (1959); **34**, 120 (1961).

[5]K. Rätzke, P. W. Hüppe, and F. Faupel, Phys. Rev. Lett. **68**,

2347 (1992).

[6]F. Faupel, P. W. Hüppe, and K. Rätzke, Phys. Rev. Lett. **65**, 1219 (1990).

[7]J. Horváth, J. Ott, K. Pfahler, and W. Ulfert, in *Proceedings of the 6th International Conference on Rapidly Quenched Metals,* 1987 [Mater. Sci. Eng. A **97**, 409 (1988)]; K. Pfahler, Ph.D. thesis, University of Stuttgart, 1987 (unpublished).

[8]H. Kronmüller and W. Frank, Radiat. Eff. Defects Solids **108**, 81 (1989).

[9]Y. Limoge, Acta Metall. **38**, 1733 (1990).

[10]H. Schröder, K. Samwer, and U. Köster, Phys. Rev. Lett. **54**, 197 (1985).

[11]R. S. Averback and H. Hahn, Phys. Rev. B **37**, 10 383 (1988).

[12]P. A. Duine, J. Sietsma, and A. van den Beukel, Acta Metall. Mater. **40**, 743 (1992).

[13]S. S. Tsao and F. Spaepen, Acta Metall. **33**, 881 (1985).

[14]C. A. Volkert and F. Spaepen, in *Proceedings of the 6th International Conference on Rapidly Quenched Metals,* 1987 [Mater. Sci. Eng. A **97**, 449 (1988)].

[15]R. C. Cammarata and A. L. Greer, in *Proceedings of the 5th International Conference on Liquid and Amorphous Metals,* 1983 [J. Non-Cryst. Solids **61&62**, 889 (1984)].

[16]O. B. Loopstra, E. R. van Snek, Th. H. de Keijser, and E. J. Mittemeijer, Phys. Rev. B **44**, 13 519 (1991).

[17]A. van den Beukel, E. Huizer, A. L. Mulder, and S. van der Zwaag, Acta Metall. **34**, 483 (1986).

[18]J. Horváth and H. Mehrer, Cryst. Latt. Def. Amorph. Mater. **13**, 1 (1986).

[19]A. van den Beukel, Scripta Metall. **22**, 877 (1988).

[20]A. Witvrouw, Ph.D. thesis, Harvard University, 1992 (unpublished).

[21]S. K. Sharma, M.-P. Macht, and V. Naundorf, Acta Metall. Mater. **40**, 2439 (1992).

[22]J. Bøttiger, K. Dyrbye, K. Pampus, B. Torp, and P. H. Wiene, Phys. Rev. B **37**, 9951 (1988).

[23]P. A. Duine, J. Sietsma, A. van den Beukel, and A. M. Vredenberg, Nucl. Instrum. Methods B **71**, 445 (1992).

[24]J. Bøttiger, K. Pampus, and B. Torp, Europhys. Lett. **4**, 915 (1987).

[25]T. E. Seidel and A. U. MacRae, Trans. TMS-AIME **245**, 491 (1969).

[26]G. Knuyt, L. M. Stals, and L. de Schepper, Philos. Mag. B **63**, 1289 (1991).

[27]P. A. Duine, J. Sietsma, and A. van den Beukel, in *Proceedings of the 7th International Conference on Rapidly Quenched Materials,* 1990 [Mater. Sci. Eng. A **133**, 649 (1991)].

[28]F. Spaepen, in *Physics of Defects,* Les Houches Lectures XXXV, edited by R. Balian *et al.* (North Holland, Amsterdam, 1981), p. 135.

[29]G. W. Koebrugge, J. Sietsma, and A. van den Beukel, Acta Metall. Mater. **40**, 753 (1992).

[30]P. Tuinstra, P. A. Duine, and J. Sietsma, in *Proceedings of the 8th International Conference on Liquid and Amorphous Metals,* Vienna, 1992 [J. Non-Cryst. Solids **156-158**, 519 (1993)].

[31]E. Rössler, Phys. Rev. Lett. **65**, 1595 (1990).